Power-spectrum characterization of the continuous Gaussian ensemble

A. Relaño,[1,*] L. Muñoz,[2] J. Retamosa,[2] E. Faleiro,[3] and R. A. Molina[1]
[1]*Instituto de Estructura de la Materia, CSIC, Serrano, 123, E-28006 Madrid, Spain*
[2]*Departamento de Física Atómica, Molecular y Nuclear, Universidad Complutense de Madrid, E-28040 Madrid, Spain*
[3]*Departamento de Física Aplicada, E.U.I.T. Industrial, Universidad Politécnica de Madrid, E-28012 Madrid, Spain*
(Received 4 May 2007; revised manuscript received 21 December 2007; published 4 March 2008)

The continuous Gaussian ensemble, also known as the ν-*Gaussian* or ν-*Hermite* ensemble, is a natural extension of the classical Gaussian ensembles of real ($\nu=1$), complex ($\nu=2$), or quaternion ($\nu=4$) matrices, where ν is allowed to take any positive value. From a physical point of view, this ensemble may be useful to describe transitions between different symmetries or to describe the terrace-width distributions of vicinal surfaces. Moreover, its simple form allows one to speed up and increase the efficiency of numerical simulations dealing with large matrix dimensions. We analyze the long-range spectral correlations of this ensemble by means of the δ_n statistic. We derive an analytical expression for the average power spectrum of this statistic, $\overline{P_k^{\delta}}$, based on approximated forms for the two-point cluster function and the spectral form factor. We find that the power spectrum of δ_n evolves from $\overline{P_k^{\delta}} \propto 1/k$ at $\nu=1$ to $\overline{P_k^{\delta}} \propto 1/k^2$ at $\nu=0$. Relevantly, the transition is not homogeneous with a $1/f^{\alpha}$ noise at all scales, but heterogeneous with coexisting $1/f$ and $1/f^2$ noises. There exists a critical frequency $k_c \propto \nu$ that separates both behaviors: below k_c, $\overline{P_k^{\delta}}$ follows a $1/f$ power law, while beyond k_c, it transits abruptly to a $1/f^2$ power law. For $\nu>1$ the $1/f$ noise dominates through the whole frequency range, unveiling that the $1/f$ correlation structure remains constant as we increase the level repulsion and reduce to zero the amplitude of the spectral fluctuations. All these results are confirmed by stringent numerical calculations involving matrices with dimensions up to 10^5.

DOI: 10.1103/PhysRevE.77.031103 PACS number(s): 05.45.Mt, 02.10.Yn, 24.60.−k

I. INTRODUCTION

Random matrix theory (RMT) emerged in the late 1920s when statisticians introduced the first type of random matrix ensembles (RMEs), known as Wishart ensembles [1]. Since then, RMT has been applied in physics, multivariate statistics, combinatorics, graph theory, number theory, biology, genomics, and wireless communications (see Chap. 2 of Ref. [2] and references therein).

As far as physics is concerned, RMT appeared in the mid-1950s for the first time. It was introduced by Wigner in order to circumvent the lack of a dynamical theory of the nucleus at that time [3]. According to him, the Hamiltonian which governs the behavior of a complicated system can be represented by a random matrix with no particular properties, except for the corresponding to the symmetries of the system. Most references of the first historical period can be found in [4].

The basic concepts of the theory as well as its mathematical formulation were developed in the period 1950–1963. Later, the theory was consolidated as many experimental data were gathered, like the Ericsson's cross-section fluctuations or the nuclear data ensemble. Around 1984, two developments took place which led to an exponential development of the theory: the adoption of Efetov's supersymmetry method and the ensuing coalescence of RMT and localization theory and the link between RMT and the spectral fluctuation properties of quantum systems with a chaotic classical analog. A comprehensive review of the most important concepts and developments of RMT in quantum physics can be found in [5].

We deal in this paper with the continuous Gaussian ensemble, which can be seen as a generalization of the classical Gaussian ensembles. It was first studied as a theoretical joint eigenvalue distribution, with applications in lattice gas theory (here the continuous parameter is the inverse temperature of a Coulomb gas with logarithmic potential) [6], but recently it has been found that this eigenvalue distribution can be derived from an ensemble of random matrices [7]. The actual form of this ensemble emerged from the tridiagonal representation of the three classical Gaussian ensembles: Gaussian orthogonal ensemble (GOE−$\nu=1$), Gaussian unitary ensemble (GUE−$\nu=2$), and Gaussian symplectic ensemble (GSE−$\nu=4$). This representation is amazingly simple: the matrix entries are mutually independent and real, the diagonal elements are normal random variables, and the nondiagonal are distributed according to χ distributions. Although this representation was obtained for $\nu=1$, 2, and 4, it is well defined for every value $\nu>0$, leading to the ν-Gaussian ensemble. At present, some of the most relevant results known for this ensemble are the following: (i) its eigenvalue joint distribution has the same functional form as the classical ensembles, but ν can take any real positive value, (ii) analytical expressions for average moments and the variances of the matrix traces (defined below) are available in the thermodynamic limit, (iii) the average eigenvalue density exhibits a very strong semicircle law, and (iv) the nearest-neighbor spacing distribution has proved to be successfully described by generalized γ distributions through the whole range of ν values [8].

For many years the pattern of thinking was that the RME classification was discrete. However, there were some hints suggesting that the parameter ν is actually continuous. Gaussian and circular ensembles exhibit eigenvalue repul-

*armando@iem.cfmac.csic.es

sion: two nearby eigenvalues "repeal" each other with a certain intensity. The nearest-neighbor spacing distribution $P(s)$ is widely accepted as a valid statistic to study the short-range correlations of the spectrum of a quantum system. It gives the probability that the distance between two consecutive eigenvalues, measured in units of the local average spacing, lies between s and $s+ds$. Actually, $P(s) \propto s^{\nu}$ when $s \ll 1$: this means that the probability of finding two neighboring eigenvalues at a distance s is proportional to s^{ν}, provided that s is small enough. Therefore, the dimension ν of the field over which the matrix entries are distributed measures the repulsion between consecutive eigenvalues. Since Gaussian or circular ensembles describe the spectral fluctuation properties of chaotic quantum systems, it is usually said that these systems show level repulsion. On the contrary, for generic integrable systems energy levels behave as noncorrelated random variables and $P(s) \simeq 1$ when $s \ll 1$; consequently, the parameter ν can be taken as zero for these systems. It is very interesting to observe that in the transition from an integrable to a chaotic regime, $P(s) \propto s^{\nu}$ for s small enough, with ν ranging from $\nu=0$ to $\nu=1$, 2, or 4 depending on the symmetries of the system. Thus, we are faced with the fact that the parameter ν varies in a continuous way through the whole transition.

Another hint for the existence of a continuous parameter ν comes from the analogy between the eigenvalue distribution of the classical ensembles and the free energy of a static Coulomb gas in one dimension. The parameter ν is directly related to the temperature of the gas as $\nu=1/T$. This analogy helps one to understand the fluctuation properties of these ensembles and triggers the idea that other ensembles with $\nu \neq 1$, 2, or 4 may exist. Moreover, the spacings between gas particles follow the same distribution $P(s)$ of the energy level spacings of quantum systems through the order to chaos transition [9].

There also exists a link between the continuous Gaussian ensemble and a system of identical quantum particles interacting in one dimension by a two-body potential $V(r)=g/r^2$—the so-called Calogero-Sutherland model [10]. When the particles move along a ring of length L, the wave function of the ground state is $\Psi \propto \Pi_{j<i} |\exp(i\theta_j) - \exp(i\theta_i)|^{\nu}$ for $\theta_j > \theta_i$, where $\nu=(1+\sqrt{1+2g})/2$ and θ_i is related to the positions x_i of the particles as $\theta_i = 2\pi x_i/L$ [11]. Therefore, the probability of finding the particles around the positions $X_1, X_2, \ldots, X_N$ coincides with the eigenvalue distribution of the continuous circular ensembles. It has been recently proposed that terrace-width distributions of vicinal surfaces can be properly described by the nearest-neighbor spacings distribution $P(s)$ which arises from the ground state of the Calogero-Sutherland model [12].

We analyze the long-range spectral correlations of this ensemble by means of the δ_n statistic. We derive an analytical expression for the average power spectrum of this statistic based on approximated forms for the two-point cluster function and the spectral form factor. The agreement between the theoretical predictions and the results of detailed numerical calculations is excellent for any value of the repulsion parameter ν. Thus we conclude that, as far as the power spectrum of the δ_n statistic is concerned, the approximations used in the theoretical derivation are reasonable.

The paper is organized as follows. Section II introduces the ensembles and gives some basic results. Section III contains the main results. A theoretical expression for the δ_n power spectrum is derived and checked by means of a stringent numerical calculation. The most relevant conclusions are gathered in Sec. IV.

II. DEFINITION AND BASIC RESULTS OF THE CONTINUOUS GAUSSIAN ENSEMBLE

The joint eigenvalue distribution (JED) of the Gaussian ensembles reads as

$$P_X(X) = C_{\nu} \exp(-\lambda \langle\langle X^2 \rangle\rangle) \prod_{k<l} |X_k - X_l|^{\nu}, \tag{1}$$

where C_{ν} is an appropriate normalization constant and $\langle\langle \cdots \rangle\rangle = \Sigma_k (\cdots)_{kk}$ stands for the trace operation. The average eigenvalue density, as proved by Wigner, follows the semicircle law

$$\overline{g_H(E)} \overset{N \gg 1}{\sim} g_{s.c.}(E) = \begin{cases} \dfrac{2\lambda}{\pi\nu} \sqrt{\dfrac{\nu N}{\lambda} - E^2}, & \text{for } |E| \leq \sqrt{\dfrac{\nu N}{\lambda}}, \\ 0, & \text{for } |E| > \sqrt{\dfrac{\nu N}{\lambda}}, \end{cases} \tag{2}$$

when $N \gg 1$. In the following, we write $g_{s.c.}(E)$ to denote this law.

These expressions have been derived for the triad $\nu = 1, 2, 4$, but they can be generalized straightforwardly for arbitrary real positive values. For many years the ν-Gaussian ensemble was "only" the eigenvalue distribution defined by (1). Very recently Dumitriu and Edelman [7] have provided a tridiagonal matrix model for any ν-Gaussian distribution for every $\nu > 0$. Every tridiagonal matrix satisfies $T_{kl}=0$ if $|k-l|>1$. A very important result is that the matrix elements of the model are classical random variables (normal and χ) distributed over $\mathbb{R}$, even for $\nu=2$ or 4. We denote by $\mathcal{G}(\mu, \sigma)$ a random variable distributed according a normal distribution with mean μ and variance σ^2. Similarly, we denote by χ_r the χ distribution with r degrees of freedom [13], followed from the square root of a χ^2 random variable. Then, the matrix elements of the model are random variables given by

$$T_{kk} = \mathcal{G}\left(0, \sqrt{\frac{1}{2\lambda}}\right), \quad k = 1, 2, \ldots, N,$$

$$T_{kk+1} = \sqrt{\frac{1}{4\lambda}} \chi_{(n-k+1)\nu}, \quad k = 1, 2, \ldots, N-1, \tag{3}$$

with $\lambda, \nu \in \mathbb{R}_+$. Therefore the matrices can be written as

$$T_\nu(N) = \begin{pmatrix} \mathcal{G}\left(0, \sqrt{\frac{1}{2\lambda}}\right) & \sqrt{\frac{1}{4\lambda}}\chi_{(N-1)\nu} & & & \\ \sqrt{\frac{1}{4\lambda}}\chi_{(N-1)\nu} & \mathcal{G}\left(0, \sqrt{\frac{1}{2\lambda}}\right) & \sqrt{\frac{1}{4\lambda}}\chi_{(N-2)\nu} & & \\ & \ddots & \ddots & \ddots & \\ & & \sqrt{\frac{1}{4\lambda}}\chi_{2\nu} & \mathcal{G}\left(0, \sqrt{\frac{1}{2\lambda}}\right) & \sqrt{\frac{1}{4\lambda}}\chi_{\nu} \\ & & & \sqrt{\frac{1}{4\lambda}}\chi_{\nu} & \mathcal{G}\left(0, \sqrt{\frac{1}{2\lambda}}\right) \end{pmatrix}. \tag{4}$$

From now on, the name "ν-Gaussian" or "continuous Gaussian ensemble" corresponds to these tridiagonal, real, and symmetric matrices. There are several known results, but before we quote the most important, for our purposes it is necessary to define the following elements.

(i) The average moments of the ensemble are defined as

$$M_\nu^p(N) = \overline{\frac{\langle\langle T_\nu^p(N)\rangle\rangle}{N}}, \quad p \in \mathbb{N}_0, \tag{5}$$

with $\langle\langle A\rangle\rangle = \Sigma_i (A)_{i,i}$. They are directly related to the average eigenvalue density.

(ii) The variances $V_\nu^{pq}(N)$,

$$V_\nu^{pq}(N) = \overline{\langle\langle T_\nu^p(N)\rangle\rangle\langle\langle T_\nu^q(N)\rangle\rangle} - \overline{\langle\langle T_\nu^p(N)\rangle\rangle}\,\overline{\langle\langle T_\nu^q(N)\rangle\rangle}, \quad p,q \in \mathbb{N}_0, \tag{6}$$

which are related to the two-point correlation measures of the ensemble.

We enumerate some of the most important features of the ν-Gaussian ensemble, which will be used later.

(i) The JED of the model is exactly given by Eq. (1).

(ii) The expressions of the average moments and the variances are known in the limit $N \to \infty$. Setting the normalization constant to $\lambda = \nu N$ they are given by

$$M_\nu^p(\infty) = \begin{cases} \dfrac{\Gamma(p/2 + 1/2)}{\sqrt{\pi}\Gamma(q/2 + 2)}, & \text{if } p \text{ is even}, \\ 0, & \text{if } p \text{ is odd}, \end{cases} \tag{7}$$

$$V_\nu^{pq}(\infty) = \begin{cases} \dfrac{1}{\nu}\dfrac{(p+\delta)(q+\delta)}{2^{p+q}(p+q)}\binom{p}{\frac{p+\delta}{2}}\binom{q}{\frac{q+\delta}{2}}, & \text{if } p+q = \text{even} > 0, \\ 0, & \text{otherwise}, \end{cases} \tag{8}$$

where $\delta = 0$ if $p = q = 0 \pmod 2$ and $\delta = 1$ if $p = q = 1 \pmod 2$. It is quite remarkable that, once the normalization $\lambda = \nu N$ is set, the asymptotic behavior of the moments does not depend on ν, and therefore the average eigenvalue density is the same for all $\nu > 0$ values. Moreover, $V_T^{pq}/N^2 \to 0$ when $N \to \infty$, giving rise to level ergodicity in the manner of Pandey [14]—i.e., $\mathrm{var}[g_T(E)]/\overline{g_T(E)}^2 \to 0$.

(iii) Actually, these ensembles exhibit a stronger semicircle law: not only $\overline{g_T(E)} \overset{N \gg 1}{\sim} g_{s.c.}(E)$, but with probability 1, $g_T(E)/g_{s.c.}(E) \overset{N \to \infty}{\to} 1$, for any matrix of the ensemble. Note that this result is stronger than the usual ergodicity, as quoted in the previous item.

(iv) The short-range correlations of the ν-Gaussian ensemble have been studied very recently [8]. A detailed numerical analysis shows that the $P(s)$ distribution is successfully described by generalized gamma (GG) distributions. They account both for the level repulsion in $\sim s^\nu$ when $s \to 0$ and for the whole shape of the distribution through the whole range of s values accessible to experiment or numerics. The GG distribution reduces essentially to the Wigner surmise when $\nu > \sim 2$, while it improves its accuracy for $\nu < 2$. In particular, the GG distribution describes significantly

better the $P(s)$ distribution of GOE ($\nu=1$) than the Wigner surmise and it works much better than the Brody distribution for $0\leq\nu\leq 1$ as well.

III. SPECTRAL ANALYSIS OF THE ν-GAUSSIAN ENSEMBLE

A. δ_n statistic

In order to characterize correlations of different length, we use the δ_n statistic, which is defined by

$$\delta_n = \langle \delta_{n,s} \rangle = \langle x_{s+n+1} - x_s - n \rangle, \quad n = 1, \ldots, N-1. \tag{9}$$

Here, the angular brackets denote the running average over the starting points x_s. If we place the ground state in the starting point x_s, $\delta_{n,s}$ represents the deviation of the excitation energy of the $(n+1)$th unfolded level from its average value n. In spite of some peculiarities, the function δ_n has a formal similarity with a time series [15], and actually, using numerical techniques borrowed from time series analysis, we can study long-range spectral correlations. The simplest method is the computation of the power spectrum of the δ_n series, given by

$$P_k^{\delta} = \langle |\hat{\delta}_{k,s}|^2 \rangle, \tag{10}$$

where $\hat{\delta}_{k,s}$ is the Fourier transform of $\delta_{n,s}$:

$$\hat{\delta}_{k,s} = \frac{1}{\sqrt{N}} \sum_n \delta_{n,s} \exp\left(-\frac{2\pi i k n}{N}\right). \tag{11}$$

Using RMEs, atomic nuclei, and quantum billiards, it was numerically shown [15] that the spectral rigidity of chaotic systems with $\nu=1$, 2, or 4 give rises to the following power spectra of the δ_n:

$$\overline{P_k^{\delta}} \sim \frac{N}{2\nu\pi^2 k}, \quad \nu = 1,2,4, \tag{12}$$

whenever $k \ll N$ and $N \gg 1$. Thus, the three ensembles, corresponding to different space-time symmetries, and characterized by different level repulsions, exhibit the same long-range structure in their fluctuations: in all cases the functional dependence of $\overline{P_k^{\delta}}$ is the same and without any privileged scale. We can say that these spectra, considered as time series, exhibit $1/f$ noise and therefore are completely antipersistent. On the contrary, uncorrelated spectra exhibit $1/f^2$ noise,

$$\overline{P_k^{\delta}} \sim \frac{N^2}{4\pi^2 k^2}, \quad k \ll N, \quad N \gg 1, \tag{13}$$

and behave like neither an antipersistent nor a persistent time series.

It is possible to derive a theoretical expression for $\overline{P_k^{\delta}}$ in the RMT framework. For very general ensembles the power spectrum of δ_n and the spectral form factor are related as [16]

$$\overline{P_k^{\delta}} \overset{N\gg 1}{\sim} \sum_{q\in\mathbb{Z}} \frac{N^2}{4\pi^2} \frac{K(k/N+q)}{(k+qN)^2} + \Delta, \quad 0 < k < \lfloor N/2 \rfloor, \tag{14}$$

where $\lfloor \cdots \rfloor$ stands for the floor function and $K(\tau)$ is the spectral form factor given by

$$K(\tau) = \left\langle \lim_{L\to\infty} \frac{1}{2L} \left| \int_{-L}^{L} d\epsilon\, \tilde{\rho}(\epsilon) e^{-2\pi i \epsilon \tau} \right|^2 \right\rangle, \tag{15}$$

which can be rewritten in terms of the two-point cluster function $Y_2(\epsilon)$ as

$$K(\tau) = 1 - \int_{-\infty}^{\infty} ds\, Y_2(s) \exp(-2\pi i s \tau). \tag{16}$$

The additive parameter Δ takes into account the discrete nature of the δ_n function. It depends on the difference between the variances of δ_q and $\tilde{n}(\epsilon)|_{\epsilon=q}$, whose large-$q$ behavior is [17]

$$\overline{\delta_q^2} - \overline{\tilde{n}(q)^2} = \frac{1}{3}\int_{-\infty}^{\infty} dr\, ds\, Y_3(0,r,s) - \frac{1}{2}\left(\int_{-\infty}^{\infty} dr\, Y_2(r)\right)^2, \quad q \gg 1, \tag{17}$$

except in the rare cases where the integrals do not exist. The right-hand side (rhs) is zero for Poisson and $-1/6$ for canonical ensembles. Finally, a straightforward calculation gives [16]

$$\Delta = \begin{cases} -\dfrac{1}{12} & \text{for Gaussian ensembles,} \\ 0 & \text{for Poisson ensembles.} \end{cases} \tag{18}$$

When $k \ll N$, Eq. (14) can be simplified as

$$\overline{P_k^{\delta}} \overset{N\gg 1}{\sim} \frac{N^2}{4\pi^2} \frac{K(k/N)}{k^2}, \tag{19}$$

recovering an almost exact two-point function in this limit. Since the spectral form factor of the Gaussian ensembles is $K(k/N)=2k/(\nu N)$ if $k \ll N$ and it is $K(k/N)=1$ for the Poisson ensembles, the foregoing expression reduces to Eqs. (12) and (13).

B. Derivation of $\overline{P_k^{\delta}}$ for the ν-Gaussian ensemble

1. $Y_{2\nu}$ and $K_{\nu}(\tau)$ functions

The main goal of this paper is to characterize the long-range spectral correlations of the ν-Gaussian ensemble by means of $\overline{P_k^{\delta}}$. Any derivation of this statistic needs as an intermediate step the expression of the spectral form factor $K_{\nu}(\tau)$, which is the Fourier transform of the two-point cluster function. To obtain $Y_{2\nu}$ from the variances V_{ν}^{pq} we consider the density-density correlator

$$S^g(E_1,E_2) = \overline{g(E_1)g(E_2)} - \overline{g(E_1)g(E_2)} \tag{20}$$

and calculate its Fourier transform

$$\mathcal{F}[S^g](\hat{t}) = \int \int_{\mathbb{R}^2} \exp(i\hat{E}\cdot\hat{t}) S^g(E_1,E_2) dE_1 dE_2, \quad (21)$$

where $\hat{E}=(E_1,E_2)$ and $\hat{t}=(t_1,t_2)$. Expanding the exponential it is easy to obtain the following expression in terms of the variances $V^{pq}(N)$:

$$\mathcal{F}[S^g](\hat{t}) = \sum_{\substack{p,q=0 \\ (p+q=\text{even})}}^{\infty} \frac{(it_1)^p}{p!}\frac{(it_2)^q}{q!} V^{pq}(N). \quad (22)$$

For $N=\infty$ the variances V_ν^{pq} of the ν-Gaussian ensemble can be written as

$$V_\nu^{pq}(\infty) = \frac{1}{2^{p+q-1}\nu} \sum_{[k]=1}^{min(p,q)} k \binom{p}{\frac{p-k}{2}} \binom{q}{\frac{q-k}{2}}, \quad p+q=\text{even}, \quad (23)$$

where $[k]$ stands for the restriction of k to values with the same parity of p and q. While this result is valid for $N=\infty$, we need to consider N large but finite in order to unfold the spectrum later. To circumvent this problem we introduce a cutoff $\Lambda(\nu,N)=O(N)$ such that $V_\nu^{pq}(N) \simeq V_\nu^{pq}(\infty)$ whenever $p,q \leq \Lambda$. Then

$$\mathcal{F}[S_\nu^g](\hat{t}) = \frac{2}{\nu} \sum_{\substack{p,q=0 \\ (p+q=\text{even})}}^{\Lambda} \frac{(it_1)^p}{2^p p!}\frac{(it_2)^q}{2^q q!} \sum_{[k]=1}^{min(p,q)} k \binom{p}{\frac{p-k}{2}} \binom{q}{\frac{q-k}{2}}. \quad (24)$$

Some straightforward algebra allows us to write

$$\mathcal{F}[S_\nu^g](\hat{t}) = \frac{2}{\nu} \sum_{k=0}^{\Lambda} (-1)^k k J_k(t_1) J_k(t_2), \quad (25)$$

where J_k are Bessel functions of the first kind. Inverting the Fourier transform will provide us the function $S^g(E_1,E_2)$. Indeed, if we use the following result from Ref. [18],

$$\mathcal{F}^{-1}[J_k](E) = \frac{1}{2\pi}\int_{\mathbb{R}} \exp(-iEt) J_k(t) dt = \begin{cases} \frac{(-i)^k u_k(E)}{\pi(1-E^2)^{1/2}}, & \text{for } |E|<1, \\ 0, & \text{for } |E|>1, \end{cases} \quad (26)$$

where u_k are Tchebyshev polynomials of the first kind, the density-density correlator reads

$$S_\nu^g(E_1,E_2) = \frac{2}{\pi^2\nu} \sum_{k=0}^{\Lambda} k \frac{u_k(E_1)u_k(E_2)}{(1-E_1^2)^{1/2}(1-E_2^2)^{1/2}}, \quad (27)$$

provided that we restrict ourselves to the interval $|E_1|,|E_2|<1$.

At this point the spectrum must be unfolded to get the correlations among the energy levels of a quasiuniform spectrum. For levels inside of the interval $|E_1|,|E_2|<1$ we have

$$S_\nu^\rho(\epsilon_1,\epsilon_2) = \frac{S^g(E_1,E_2)}{g(E_1)g(E_2)} = \frac{1}{2\nu N^2} \sum_{k=0}^{\Lambda} k \frac{u_k(E_1)u_k(E_2)}{(1-E_1^2)(1-E_2^2)} \quad (28)$$

for the density-density correlator in the unfolded energy scale.

In order to discard the self-correlation term $\delta(\epsilon_1-\epsilon_2)$, which is always included in $S_\nu^\rho(\epsilon_1,\epsilon_2)$, and obtain the two-point cluster function $Y_{2\nu}(\epsilon_1,\epsilon_2)=\delta(\epsilon_1-\epsilon_2)-S_\nu^\rho(\epsilon_1,\epsilon_2)$, it is convenient to perform a similar expansion of the δ function. In terms of Tchebyshev polynomials of the second kind, $v_k(E)$, we can write

$$\delta(\epsilon_1-\epsilon_2) = \frac{1}{N} \sum_{k=0}^{\Lambda} v_k(E_1) v_k(E_2). \quad (29)$$

Before proceeding to the explicit calculation of the sums (27) and (29), it is important to recall that very often correlations decay to zero on an energy scale of the order of $\bar{S}$. Since $\bar{S}=O(1/N)$, the relevant scale for the difference of the two energies in question is really small, $E_2-E_1=O(1/N)$, giving rise to an unfolded spacing $s=O(N\Delta E)=O(1)$.

With these considerations in mind and using the fact that $\Lambda(\nu,N)=O(N)\gg 1$, it is indeed easy to transform the expansions of $S_\nu^\rho(\epsilon_1,\epsilon_2)$ and $\delta(\epsilon_1-\epsilon_2)$ into integrals. Particularly, the two-point cluster function reads

$$\begin{aligned} Y_{2\nu}(\epsilon_1,\epsilon_2) &= \delta(\epsilon_1-\epsilon_2) - S_\nu^\rho(\epsilon_1,\epsilon_2) \\ &\overset{N\gg 1}{\sim} \frac{\Lambda}{2N}\int_0^1 \cos(\Lambda\Delta E x) dx \\ &\quad - \frac{1}{\nu}\left(\frac{\Lambda}{2N}\right)^2 \int_0^1 x\cos(\Lambda\Delta E x) dx. \end{aligned} \quad (30)$$

An inspection of both integrals shows that an exact cancellation of the self-correlation term occurs only for $\Lambda(\nu,N)=2\nu N$. Then $Y_{2\nu}$ can be written as

$$\begin{aligned} Y_{2\nu}(\epsilon_1,\epsilon_2) &\overset{N\gg 1}{\sim} \nu \int_0^1 (x-1)\cos(2\nu N\Delta E x) dx \\ &= 2\nu \left(\frac{\sin(\nu N\Delta E)}{2\nu N\Delta E}\right)^2, \end{aligned} \quad (31)$$

and taking into account that $s=\epsilon_2-\epsilon_1=\overline{g\left(\frac{E_1+E_2}{2}\right)}\Delta E \overset{N\gg 1}{\sim} 2N\Delta E/\pi$, the cluster function reads

$$Y_{2\nu}(s) \overset{N\gg 1}{\sim} \frac{2}{\nu}\left(\frac{\sin[\pi\nu s/2]}{\pi s}\right)^2. \quad (32)$$

Exact analytical expressions of the cumulant $Y_2(s)$ are known for the three classical Gaussian ensembles, GOE($\nu=1$), GUE($\nu=2$), and GSE($\nu=4$) [19]. One immediately realizes that Eq. (32) differs from the expression of $Y_2(s)$ for GOE and GSE. Thus, it is only an approximated form and we should discuss its validity for different values of ν. Before proceeding further, it will be profitable to pause and

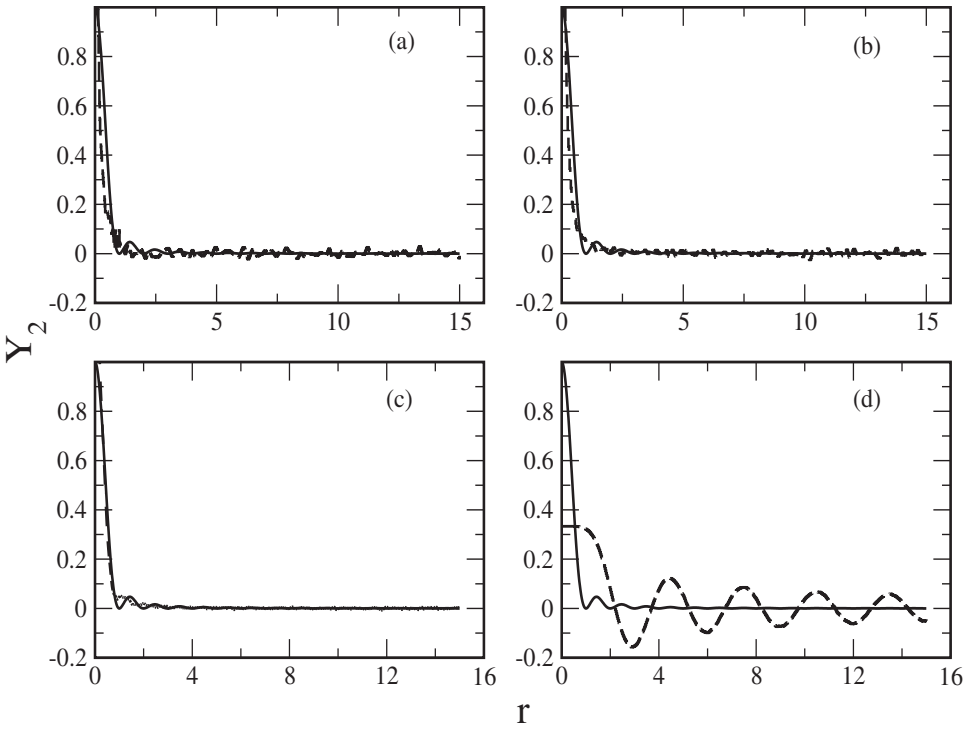

FIG. 1. Numerical estimation of $\hat{Y}_{2\nu}^{\text{exact}}(r)$ (dashed lines) compared to the approximated theoretical expression $Y_{2,\nu=2}$ (solid lines) for (a) $\nu=0.1$, (b) $\nu=0.5$, (c) $\nu=1.6$, and (d) $\nu=6.0$.

recall that our objective is not the cluster function, but the power spectrum of δ_n. Although the former is a direct measure of the two-point spectral fluctuations, it is very difficult to compute from an experimental or numerical spectrum. For this reason one generally considers other statistics like $\Sigma_\nu^2(s)$, $\overline{\Delta_{3\nu}(s)}$, or $\overline{P_{k\nu}^\delta}$, which are easier to compute. All these measures are different types of integral transforms of $Y_{2\nu}$, and therefore the comparison between the exact form and our approximation must emphasize the features that may influence the behavior of these integrals.

An inspection of Eq. (32) reveals that ν modulates the fluctuations of the cluster function: the characteristic "period" of these fluctuations is given by $\Delta s_\nu = 4\pi/\nu$. Thus, in order to render the comparison of the influence of Y_2 for different values of ν meaningful, one should consider intervals of the same length in units of Δs_ν. If we introduce the new variable $r=\nu s/2$, the previous statement is equivalent to using intervals with fixed length Δr. Performing the change of variable the three statistics mentioned above can be easily written as

$$\Sigma_\nu^2(s) = \frac{2}{\nu}\left[r - \int_0^r dx (r-x)\left(\frac{2}{\nu} Y_{2\nu}(2x/\nu)\right)\right], \tag{33}$$

$$\overline{\Delta_{3\nu}(s)} = \frac{2}{\nu}\left[\frac{r}{15} - \frac{1}{15r^4}\int_0^r dx (r-x)^3 (2r^2 - 9rx - 3x^2) \times \left(\frac{2}{\nu} Y_{2\nu}(2x/\nu)\right)\right], \tag{34}$$

$$K_\nu(\tau) = 1 - \int_{\mathbb{R}} dx \left(\frac{2}{\nu} Y_{2\nu}(2x/\nu)\right) \exp[-2\pi i r(2\tau/\nu)]. \tag{35}$$

Therefore, the relevant function in the new scale is

$$\hat{Y}_{2\nu}(r) = \frac{2}{\nu} Y_{2\nu}(2r/\nu). \tag{36}$$

In particular, our approximated function (32) takes the simple form

$$\hat{Y}_{2\nu}(r) \overset{N\gg 1}{\sim} Y_{2\nu=2}(r), \tag{37}$$

regardless of the value of ν. Combining all these ideas and results we conclude that the comparison between the exact and approximated forms of the cluster function is given by

$$\hat{Y}_{2\nu}^{\text{exact}}(r) \overset{?}{=} \hat{Y}_{2\nu}(r) = Y_{2\nu=2}(r), \tag{38}$$

where from now on we denote the exact cluster function by $\hat{Y}_{2\nu}^{\text{exact}}(r)$, while $\hat{Y}_{2\nu}(r)$ stands for the approximated form (37).

Figure 1 displays the comparison between numerical estimations of $\hat{Y}_{2\nu}^{\text{exact}}(r)$ and $Y_{2\nu=2}(r)$ for several values of ν ($\nu=0.1, 0.5, 1.6, 6$). For $\nu<2$ the theoretical approximation reproduces reasonably well the main trend of the exact form, although there are some discrepancies. The former exhibits a damped fluctuation component of characteristic length $\Delta r \approx 1$, which is not present in the former. Moreover, the behavior of the two forms is different at the origin; while the approximation $Y_{2\nu=2}(r)$ always tends to unity, the numerical results approach $2/\nu$ instead. The magnitude of the difference is quite large for $\nu \ll 1$, but it always decays so quickly that it becomes negligible for quite small values of r. The effect on fluctuation measures like $\Sigma_\nu^2(s)$ or $\overline{\Delta_{3\nu}(s)}$ is relatively small: the asymptotic behavior of the theoretical expressions derived from Eq. (37) agrees with the numerical values, except for a constant. As previously commented we focus on the power spectrum of the δ_n statistic, which is

related to the spectral form factor. Since $K_\nu(\tau)$ is very sensitive to the fluctuation structure of Y_2, its behavior will also be disturbed. However, taking into account that characteristic lengths of conjugate variables are in inverse order, it is easy to realize that the trend of $K_\nu(\tau)$ will be well reproduced by our approximation (at least) for $\tau \leq \nu/2$. Translating this result to the power spectrum of δ_n, we do not expect the theoretical predictions to exhibit large deviations from the numerical values up to $k=N\nu/2$.

When $\nu>2$ the comparison between the approximated and exact forms of Y_2 looks worse. The numerical (exact) values fluctuate around the theoretical curve with a characteristic length of order $\nu/2$ and amplitudes that decay very slowly from an initial value $2/\nu$ as r increases. Surprisingly, it may appear that the influence of this discrepancy on the usual statistics is very limited. Similarly to the previous case, the slope of the theoretical estimations of $\Sigma^2_\nu(s)$ or $\overline{\Delta_{3\nu}(s)}$ is correct and the deviation from the numerical values is quite small. Nevertheless, since these measures take very small values, the relative error is large. On the other hand, the limitations of $\hat{Y}_{2\nu}(r)$ do not produce in this case noticeable effects on $\overline{P^\delta_k}$. The reason is that fluctuations of characteristic length $\Delta r \approx \nu/2$ can only manifest in $\overline{P^\delta_k}$ for values of $k \geq N$, which are far beyond the interval $[1, N/2]$ where the discrete Fourier transform of δ_n is defined.

The spectral form factor $K(\tau)$ is the following integral transform of the two-point cluster function,

$$K(\tau) = 1 - \int_{-\infty}^{\infty} ds\ Y_2(s)\exp(-2\pi i s\tau), \tag{39}$$

and using Eq. (32), one obtains

$$K_\nu(\tau) = \begin{cases} \dfrac{2|\tau|}{\nu}, & \text{for } |\tau| \leq \dfrac{\nu}{2}, \\ 1, & \text{for } |\tau| > \dfrac{\nu}{2}. \end{cases} \tag{40}$$

Similarly to the case of $Y_{\nu 2}$, this result is exact only for $\nu=2$. For discrete values of τ, the replacement $\tau \to k/N$ leads to

$$K_\nu(k/N) = \begin{cases} \dfrac{2|k|}{\nu N}, & \text{for } \dfrac{|k|}{N} \leq \dfrac{\nu}{2}, \\ 1, & \text{for } \dfrac{|k|}{N} > \dfrac{\nu}{2}. \end{cases} \tag{41}$$

2. Closed expression for $\overline{P^\delta_{\nu k}}$

A final comment about the calculation of $\overline{P^\delta_{\nu k}}$ is in order. It concerns the last term of Eq. (14). As was previously shown, it depends on the two-point as well as on the three-point cumulant, but the lack of an analytical expression for $Y_{3\nu}$ makes the calculation of this term impossible. This will have consequences in the high-frequency region, where the value of Δ becomes more relevant. We shall quantify the relevance of this approximation when comparing with numerics.

Having commented on the limitations we may encounter when using Eq. (37), we proceed now to deduce a closed expression for $P^\delta_{\nu k}$. Obviously, the nonanalyticity of $K_\nu(\tau)$ at $k=\nu N/2$ propagates to the power spectrum of δ_n. To account for its effect we consider separately the cases where ν pertains to the intervals $(0,1),[1,2),\ldots,[l,l+1)$, etc. We furnish some examples that will help one to understand the general case.

(i) $\nu \in (0,1)$. In this case all the terms of Eq. (14), except those with $q=0$, satisfy $|q+k/N| > \nu/2$. Inasmuch as the series

$$\frac{N^2}{4\pi^2}\sum_{q\in\mathbb{Z}}\frac{1}{(k+qN)^2} = \frac{1}{4\sin^2\left(\dfrac{\pi k}{N}\right)}, \tag{42}$$

$\overline{P^\delta_{\nu k}}$ admits a closed expression

$$\overline{P^\delta_{\nu k}} \overset{N\gg 1}{\sim} \frac{N^2}{4\pi^2}\frac{K_\nu(k/N)-1}{k^2} + \frac{1}{4\sin^2\left(\dfrac{\pi k}{N}\right)}, \quad 0 < k \leq \lfloor N/2 \rfloor. \tag{43}$$

(ii) $\nu \in [1,2)$. Here, we note that only the terms with $q=0$ and $q=-1$ are smaller than or equal to $\nu/2$. Taking into account that the spectral form factor is an even function—i.e., $K(\tau)=K(-\tau)$—the power spectrum becomes

$$\overline{P^\delta_{\nu k}} \overset{N\gg 1}{\sim} \frac{N^2}{4\pi^2}\left[\frac{K_\nu(k/N)-1}{k^2} + \frac{K_\nu(1-k/N)-1}{(N-k)^2}\right] + \frac{1}{4\sin^2\left(\dfrac{\pi k}{N}\right)}, \quad 0 < k \leq \lfloor N/2 \rfloor. \tag{44}$$

(iii) $\nu \in [2,3)$. The distinctive terms correspond in this case to $q=0,1$ in the positive side and $q=-1,-2$ in the negative one.

These particular cases show us the general pattern when $\nu \in [l, l+1)$. It is given by

$$\overline{P^\delta_{\nu k}} \overset{N\gg 1}{\sim} \frac{N^2}{4\pi^2}\left[\sum_{q=0}^{\lfloor l/2 \rfloor}\frac{K_\nu(k/N+q)-1}{(k+qN)^2} + \sum_{q=1}^{\lfloor l+1/2 \rfloor}\frac{K_\nu(q-k/N)-1}{(qN-k)^2}\right] + \frac{1}{4\sin^2\left(\dfrac{\pi k}{N}\right)}, \quad 0 < k \leq \lfloor N/2 \rfloor. \tag{45}$$

Of special interest among the different intervals is the case $\nu \in (0,1]$ because it may characterize the transition of certain systems from a regular to a chaotic dynamics. Indeed, Eq. (43) exhibits two different behaviors depending on the value of ν:

$$\overline{P_{\nu k}^{\delta}} \overset{N\gg 1}{\sim} \begin{cases} \dfrac{N}{2\pi^2\nu k} - \dfrac{N^2}{4\pi^2 k^2} + \dfrac{1}{4\sin^2\left(\dfrac{\pi k}{N}\right)}, & k/N \le \nu/2 \le 1/2, \\ \dfrac{1}{4\sin^2\left(\dfrac{\pi k}{N}\right)}, & 1/2 \le \nu/2 < k/N. \end{cases} \tag{46}$$

Thus, there is a clear transition around $k/N=\nu/2$. For $k/N \le \nu/2$ the power spectrum shows the characteristic behavior of chaotic systems; for $k/N > \nu/2$, its behavior is that of an integrable system [15]. Moreover, if $\nu \ll 1$,

$$\overline{P_{\nu k}^{\delta}} \overset{N\gg 1}{\sim} \frac{N}{2\pi^2\nu k}, \quad k/N \le \nu/2 \ll 1, \tag{47}$$

$$\overline{P_{\nu k}^{\delta}} \overset{N\gg 1}{\sim} \frac{N^2}{4\pi^2 k^2}, \quad \nu/2 < k/N \ll 1. \tag{48}$$

For arbitrary values of ν, the number of terms increases linearly with ν; therefore, the larger the value of ν, the less compact is Eq. (45). Nevertheless, inasmuch as the frequency $k \ll N\nu$, $\overline{P_{\nu k}^{\delta}}$ admits a rather simple expression

$$\overline{P_{\nu k}^{\delta}} \overset{N\gg 1}{\sim} \frac{N}{2\pi^2\nu k}, \quad 0 < k \ll N\nu, \tag{49}$$

which unveils that, except for $\nu \approx 0$, the low-frequency region always exhibits $1/f$ correlations.

C. Numerical calculation

Now, we aim at testing whether all these expressions do describe the actual fluctuation properties of the ν-Gaussian ensemble obtained by numerical experiments. We take advantage of the tridiagonal form of these matrices, which allows us to deal with very large dimensions to obtain significant results and study finite-size effects.

Needless to say, the spectra have to be unfolded in order to remove the modulation due to the secular trend of the eigenvalue density. The smooth part of the eigenvalue density $\overline{g(E)}$ is well described by the semicircle law of Wigner, regardless of the value of ν; thus, the unfolding could be performed analytically in every case. Nevertheless, this result is exact only in the limit $N \to \infty$ and slight deviations occur for finite N. Since the δ_n statistic is very sensitive to small imperfections of the unfolding procedure, we perform a double unfolding to avoid spurious effects: first, we unfold the spectra by using Wigner's semicircle law, and afterwards we reunfold them by means of a fit to Chebyshev polynomials.

It is natural to consider the two domains $\nu < 1$ and $\nu \ge 1$ apart because systems with $\nu=1$, 2, or 4 exhibit $1/f$ noise, while regular spectra ($\nu=0$) are characterized by $1/f^2$ noise.

$0 < \nu \le 1$. Equation (46) shows the existence of a critical frequency $k_c = \nu N/2$, where the behavior of $\overline{P_k^{\delta}}$ changes abruptly. When $k < k_c$, $\overline{P_k^{\delta}} \propto 1/k$ and the spectra exhibit the characteristic pattern of chaotic quantum systems. On the contrary, for $k > k_c$, $\overline{P_k^{\delta}} \propto 1/k^2$, and therefore the spectra behave as $1/f^2$ noise, which is a fingerprint of integrable systems. Thus, $1/f$ and $1/f^2$ noises have a neat presence through the whole range of these values of ν, the former at the coarsest scales, the latter at the finest ones. This heterogeneous behavior is rather different from that found in some intermediate semiclassical systems where the power spectrum exhibits a power law $\overline{P_k^{\delta}} \propto 1/f^{\alpha}$ with $1 < \alpha < 2$ [20].

We have calculated the averages $\overline{P_k^{\delta}}$ by using samples of 20 members pertaining to ensembles with dimensions $N = 10^3, 10^4, 10^5$. In order to make possible a direct comparison of level sequences with different lengths, we plot $\overline{P_k^{\delta}}$ in terms of the dimensionless frequency $\omega = 2\pi k/N$ instead of k. The results of these calculations are depicted in Fig. 2 for $\nu = 0.001, 0.01, 0.1, 1$. The agreement between theory and numerics can be considered very good. Nevertheless, there exist some differences. The actual transition from a $1/f$ to a $1/f^2$ regime, around the critical frequency $\omega_c = \pi$, is slightly smoother than that predicted by Eq. (46); for both $\omega \gg \omega_c$ and $\omega \ll \omega_c$, our approximated formula works very well. This discrepancy is due to the approximated character of $Y_{2\nu}$ [see Eq. (32)]. The second problem concerns the points at very low frequencies $\omega \simeq 2\pi/N$, which fall far below the theoretical curve; according to our experience, this is a spurious effect due to imperfections in the unfolding procedure. As a final comment, we would like to add that the absence of the additive term Δ does not entail relevant consequences in this case; moreover, the approximated formula (48) is able to reproduce the numerical results accurately, and thus it is a simple way to characterize the transition between uncorrelated sequences with $\nu \simeq 0$ to correlated ones with $\nu \simeq 1$.

$\nu > 1$. According to Eq. (45), we expect the behavior of $\overline{P_k^{\delta}}$ to be simpler in this case. Actually, it predicts a $1/f$ noise in the low-frequency region regardless of the value of ν. We performed several simulations with samples of 20 matrices of dimension $N = 5 \times 10^4$, although we only show four cases corresponding to $\nu=2$, 5, 10, and 100. Figure 3 displays the comparison with the theoretical predictions of (45). Contrary to the previous case (where $\nu \le 1$) the relevance of the additive term Δ is not negligible and its influence increases with ν; for this reason, the theoretical curve fails to describe the numerical data at high frequencies. The insets show the difference between numerical and theoretical results in a simple logarithmic scale for the high-frequency region. We can see two important facts: (a) the absolute value of Δ decreases with ν, as is expected since for $\nu \to \infty$, $\delta_n \to 0$, but its relative importance increases; and (b) the approximated expression (49) gives a better description than the more complete (45), which allows us to conclude that the $1/f$ behavior constitutes a very good approximation for larger values of ν. In the low and intermediate regions the agreement with Eqs. (45) and (49) is amazingly good and therefore compatible with an exact $1/f$ noise.

As shown in Ref. [21] the same result is true for another family of ensembles built by applying the Lanczos algorithm and changing *ad hoc* the fluctuations of the matrix elements. Therefore, the analogy between chaotic energy spectra and a time series is substantiated: $1/f$ noise arises as the main fea-

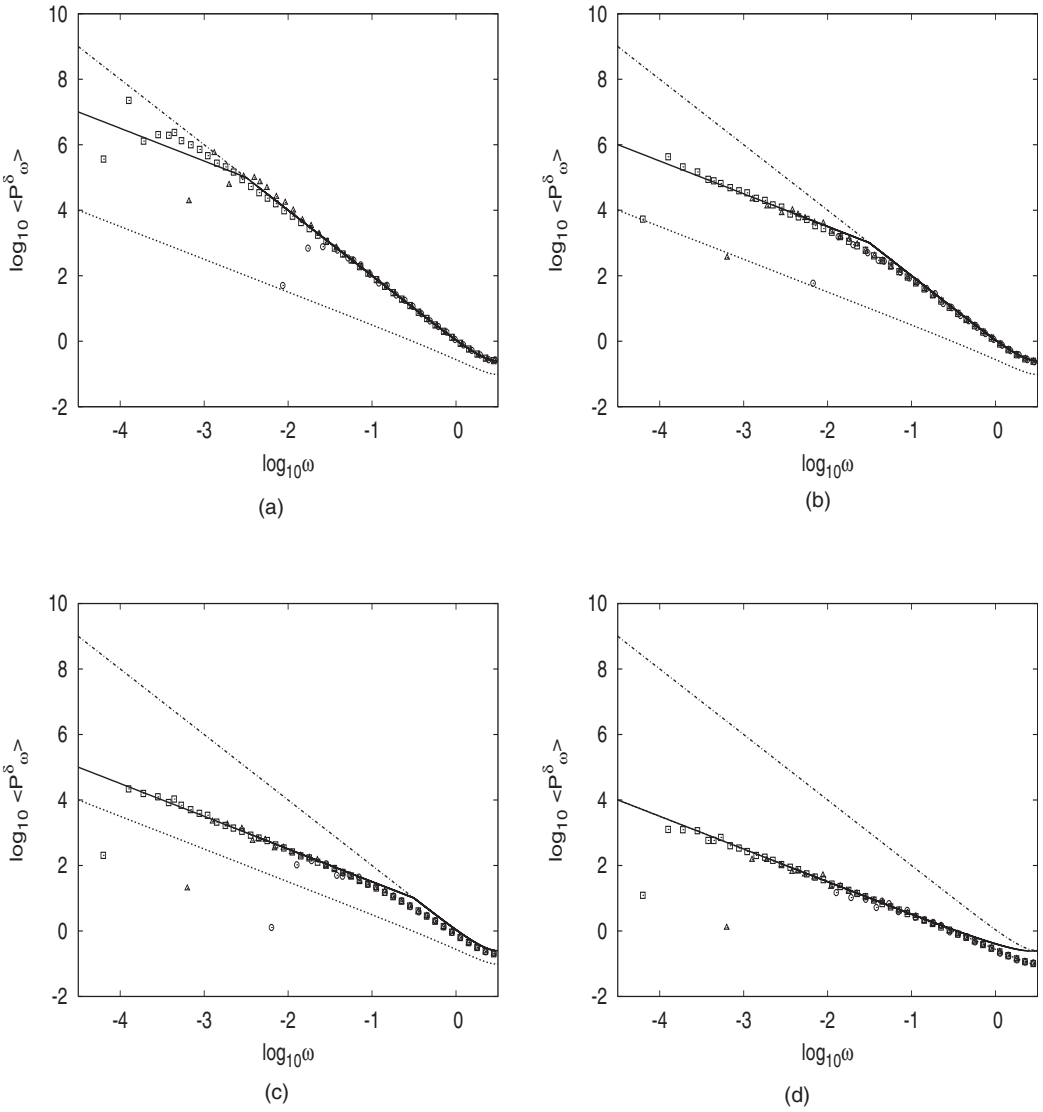

FIG. 2. Numerically calculated values of $\overline{P_k^\delta}$ plotted in double-logarithmic scale for ensembles of dimension $N=10^3$ (circles), $N=10^4$ (triangles), and $N=10^5$ (squares). Panels (a)–(d) display the results for $\nu=0.001$, $\nu=0.01$, $\nu=0.1$, and $\nu=1$. Ensemble averages are calculated by using samples of 20 matrices. The theoretical predictions of Eqs. (46), (47), and (48) are drawn as solid, dotted, and dashed lines, respectively.

ture of a transition that reduces to zero the amplitude of the spectral fluctuations, preserving its scale-free correlation structure. Moreover, the link between the repulsion parameter ν and the inverse temperature of a one-dimensional Coulomb gas, established by Eq. (1), provides a physical analogy to explain how long-range spectral fluctuations are frozen into a nonfluctuating level sequence.

IV. SUMMARY AND CONCLUSIONS

Summarizing, we have investigated the long-range spectral fluctuations of the ν-Gaussian ensemble. This random matrix ensemble is a continuous extension of the classical Gaussian ensembles ($\nu=1,2,4$), where the repulsion parameter ν can take any positive real value. One of its major characteristics is its simple tridiagonal form, which has the great advantage of an unrivaled speedup and efficiency in numerical simulations with large matrix dimensions.

We dealt with the δ_n statistic, which measures long-range spectral correlations (short-range correlations have been recently studied in [8]). Because of its formal similarity with a time series, we have used techniques borrowed from this field to obtain information on the fluctuations at all scales. It is well known that the power spectrum of δ_n exhibits $1/f^2$ noise for integrable systems ($\nu=0$) and $1/f$ noise for chaotic ones ($\nu=1,2,4$). For some intermediate systems, a $1/f^\alpha$ noise has been found, with $1<\alpha<2$, but this behavior still lacks a theoretical explanation. It has also been shown that $1/f$ noise is present in spectra with high spectral rigidity in general.

We have derived an analytical expression for the ensemble-averaged power spectrum of the δ_n statistic, $\overline{P_k^\delta}$, and compared its predictions with stringent numerical calcu-

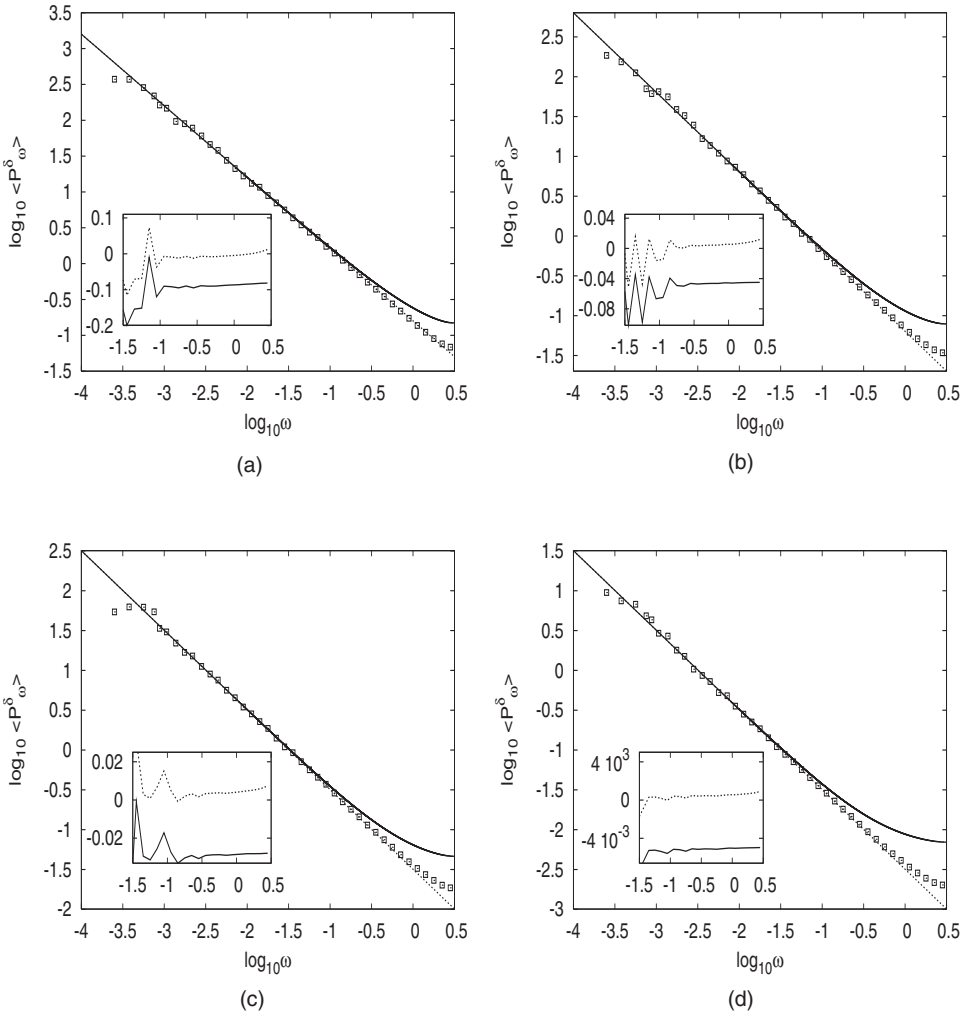

FIG. 3. Comparison of the numerical results of $\overline{P_k^\delta}$ (squares) with the predictions of Eq. (45) (solid line) and Eq. (49) (dashed line) for ensembles of dimension $N=5\times10^4$ and $\nu=2$ (a), $\nu=5$ (b), $\nu=10$ (c), and $\nu=100$ (d). The insets show the difference between the predictions and the numerical results in the high-frequency region.

lations. If $0<\nu\leq1$, the theoretical as well as the numerical values of $\overline{P_k^\delta}$ unveil a critical frequency $k_c\propto\nu$, where the long-range structure of the spectral fluctuations changes abruptly. Below k_c, the spectral fluctuations exhibit the characteristic pattern of classical Gaussian ensembles, while at higher frequencies they follow the predictions of the Poisson statistics. The evolution from GOE to Poisson statistics is heterogeneous because both $1/f$ and $1/f^2$ noises coexist through the whole transition from $\nu=0$ to $\nu=1$, and it differs from the homogeneous behavior found in other systems where a power law $\overline{P_k^\delta}\propto1/f^\alpha$ with $1<\alpha<2$ takes place at all scales. With the numerical calculations, we have confirmed this heterogeneous behavior, despite the transition from a $1/f$ to a $1/f^2$ regime being actually smoother; the critical frequency k_c is a good indicator of the scale in which this transition takes place.

When $\nu>1$ the pattern is rather different. $\overline{P_k^\delta}$ exhibits a $1/f$ power law through almost the whole frequency domain. As ν becomes larger there is a monotonic increase of the spectral rigidity that reduces dramatically the amplitude of the spectral fluctuations. In the limit $\nu\to\infty$ they fall to zero. This result substantiates the analogy between δ_n and a time series as it shows that the $1/f$ noise is the main feature along the transition from a chaotic to a picket-fence spectrum. In this case the agreement between analytical and numerical results is excellent, except in the high-frequency region, because the relevance of the constant term Δ that we dropped is not negligible here.

Note added. Recently, a numerical analysis of the continuous Gaussian ensemble, similar to ours, was published [22].

ACKNOWLEDGMENTS

This work was supported in part by Spanish Government Grants Nos. FIS2006-12783-C03-01 and FIS2006-12783-C03-02 and by Comunidad de Madrid–CSIC Grant No. 200650M012. A.R. was supported by the Spanish program "Juan de la Cierva."

[1] J. Wishart, Biometrika **10**, 32 (1928).
[2] I. Dumitriu, Ph.D. thesis, Massachussets Institute of Technology, 2003.
[3] E. P. Wigner (unpublished).
[4] C. E. Porter, *Statistical Theories of Spectra: Fluctuations* (Academic Press, New York, 1965).
[5] T. Guhr, A. Müller-Groeling, and H. A. Weidenmüller, Phys. Rep. **299**, 189 (1998).
[6] F. J. Dyson, J. Math. Phys. **3**, 1191 (1962).
[7] I. Dumitriu and A. Edelman, J. Math. Phys. **43**, 5830 (2002); I. Dumitriu and A. Edelman, Ann. Inst. Henri Poincare, Sect. A **41**, 1083 (2005).
[8] G. Le Caër, C. Male, and R. Delannay, Physica A **383**, 190 (2007).
[9] R. Scharf and F. M. Izrailev, J. Phys. A **23**, 963 (1990).
[10] F. Calogero, J. Math. Phys. **10**, 2191 (1969); **10**, 2197 (1969).
[11] B. Sutherland, Phys. Rev. A **4**, 2019 (1971); J. Math. Phys. **12**, 246 (1971).
[12] H. Gebremariam, S. D. Cohen, H. L. Richards, and T. L. Einstein, Phys. Rev. B **69**, 125404 (2004); H. L. Richards and T. L. Einstein, Phys. Rev. E **72**, 016124 (2005); A. Pimpinelli, H. Gebremariam, and T. L. Einstein, Phys. Rev. Lett. **95**, 246101 (2005); A. N. Benson, H. L. Richards, and T. L. Einstein, Phys. Rev. B **73**, 115429 (2006).
[13] Although the parameter r is named the "number of degrees of freedom," it can take any positive real value. The corresponding probability distribution $P_{\chi_r}(x)$ is well defined, and $\int dx\, P_{\chi_r}(x)dx=1$, for every $r>0$.
[14] A. Pandey, Ann. Phys. (N.Y.) **119**, 170 (1979).
[15] A. Relaño, J. M. G. Gómez, R. A. Molina, J. Retamosa, and E. Faleiro, Phys. Rev. Lett. **89**, 244102 (2002).
[16] E. Faleiro, J. M. G. Gómez, R. A. Molina, L. Muñoz, A. Relaño, and J. Retamosa, Phys. Rev. Lett. **93**, 244101 (2004).
[17] J. B. French, V. K. B. Kota, A. Pandey, and B. Tomsovic, Ann. Phys. (N.Y.) **181**, 198 (1988).
[18] *Handbook of Mathematical Formulas*, edited by M. Abramowitz and I. A. Stegun (Dover, New York, 1972).
[19] M. L. Mehta, *Random Matrices* (Academic, New York, 1991).
[20] J. M. G. Gómez, A. Relaño, J. Retamosa, E. Faleiro, L. Salasnich, M. Vranicar, and M. Robnik, Phys. Rev. Lett. **94**, 084101 (2005); M. S. Santhanam and J. N. Bandyopadhyay, *ibid.* **95**, 114101 (2005).
[21] A. Relaño, J. Retamosa, E. Faleiro, R. A. Molina, and A. P. Zuker, Phys. Rev. E **73**, 026204 (2006).
[22] C. Male, G. Le Caër, and R. Delannay, Phys. Rev. E **76**, 042101 (2007).